MODULE-LEVEL POWER ELECTRONICS UNDER INDOOR PERFORMANCE TESTS

Cyril Allenspach*, Victor Gonzalez de Echavarri Castro, Samuel Richter, Christoph Meier, Fabian Carigiet, Franz Baumgartner

ZHAW, Zurich University of Applied Sciences, School of Engineering, IEFE
www.zhaw.ch/~bauf, Technikumstr. 9, CH-8401 Winterthur, Switzerland
*phone: +41 58 934 45 76; email: alls@zhaw.ch

ABSTRACT: In the last decade, very few papers with outdoor measurement test results were published, which demonstrated a benefit of module-level power electronics (MLPE) higher than the measurement uncertainty. Due to the expected small difference in efficiency between conventional string-inverter based and MLPE systems, indoor measurements are required to exclude natural variation of solar irradiance in outdoor tests. Therefore, indoor efficiency measurements were performed on MLPE. Afterwards, the indoor measured efficiency of the single PV module DC/DC power optimizers were multiplied with the DC/AC inverter measurements. The final system efficiency with the maximum average value resulted in 94.78 % and with the power weighted efficiency in 94.37 %. Accordingly, if mismatches are neglected, the analysed MLPE system is expected to yield approximately 2.82 % less energy than a comparable string-inverter based system in unshaded conditions. However, in the case of shading, the tested system with heavy-shading orthogonal to the cell strings was estimated to yield approximately 3.5 % more energy on a clear-sky day in March in Winterthur, Switzerland. The performances determined in the tests are significantly lower than the efficiencies provided by the datasheet of the power optimizers (around -2.29 %). However, they are still presumed to provide significant additional yields for PV systems with medium- and heavy-shading conditions.
Keywords: Module-Level Power Electronics, MLPE, Power Optimiser, Efficiency, Performance, Testing, Shading

1 INTRODUCTION

Due to the electrical wiring of conventional PV systems with string inverters and their centralized maximum power point tracking (MPPT), partial-shading conditions have a great impact on the performance of such systems. A solution to the mentioned problem is the use of individual MPPT per PV module that are present in module-level power electronics (MLPE) such as microinverters or power optimizers (DC/DC-converter). One of the first applications for DC/DC-converters for PV-systems were submitted in 2001 [1]. Whereas, the today's market leader of power optimizer, namely SolarEdge Technologies Ltd and Tigo Energy Inc, applied for their patents between the years 2004 [2] and 2005 [3]. For example, SolarEdge Technologies Inc. application was granted in 2007 [2] and their first systems were sold in 2009 [4]. In 2018, only 9 years after the initial release of the mentioned PV system architecture, the global power optimizer market exceeded the size of 1 billion USD [5]. As an example, the mentioned size corresponds to approximately $1/8^{th}$ of the current global PV inverter market size [6]. Furthermore, in reference to the number of units sold, Solaredge has shipped over 45 million power optimizers and 1.5 million inverters in the 14 years since they were founded [7]. Today, they have a market share of more than 50 % within the residential PV market in the USA and they also have had a decent yearly growth of 30% in the European market in the last three years [8].

Several studies were conducted to determine the performance of MLPE in the last decade. In detail, the study results have shown that they offer a greater flexibility in the panel layout in terms of shading conditions, as well as improved protection against electric shock in installation work [9]. They offer a solution to prevent module mismatching of series connected modules in different working conditions, if the operating range of the MPPT is considered [10]. In detail, it is important that the variations of the mismatch are in the tracking range of the MLPE and the voltage after the DC/DC conversion is in a suitable range for the inverter of the system.

One of the few studies that compared a string inverter system with a power optimizer system, showed an increase in efficiency greater than the measurement uncertainties for the MLPE system [11]. However, the comparison was made between a string inverter with a transformer coupling and a MLPE system with a transformer-less inverter. Due to the iron losses in the transformer, the efficiency rating of this type is generally lower than for inverters without it [12]. As a result, the need arises to analyse the performance of MLPE with indoor measurement data and determine their effective performance. In the final analysis, the according system performance must be compared to a string inverter system with a transformer-less PV inverter.

2 POTENTIAL YIELD OF MLPE

A PV module is operated near the maximum power point, whereby the MPPT algorithm and the quality of power electronic components determine how close the system manages to approach the MPP. If the MPP in the conventional string inverter system and in the system with power optimizer are assumed to be identical in unshaded conditions (as visualised in Figure 1), only the efficiency of the DC/DC conversion will affect the yield. Consequently, the system without the additional conversion step (i.e. the system with string inverter), will receive more power from the module-level.

One of the major claims of the use of MLPE in PV systems is the reduction of system losses due to partial shading of PV modules. In detail, the mentioned losses occur when one or several modules of a PV plant are shaded in a way that they have several local MPPs and the suboptimal point is tracked (visualised in Figure 2).

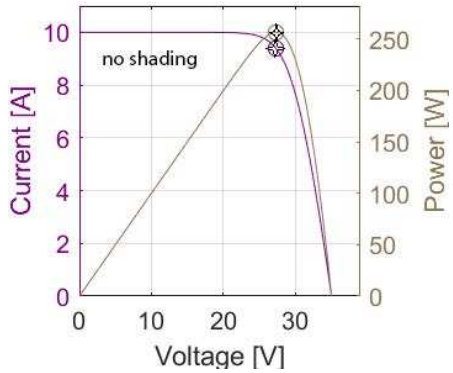

Figure 1: IV- and voltage-power-curve of a 250 Watt PV-module with three bypass-diodes in unshaded conditions. Additionally, the global I_{MPP} and P_{MPP} are visualised with circles and string-inverter system tracked MPP with stars.

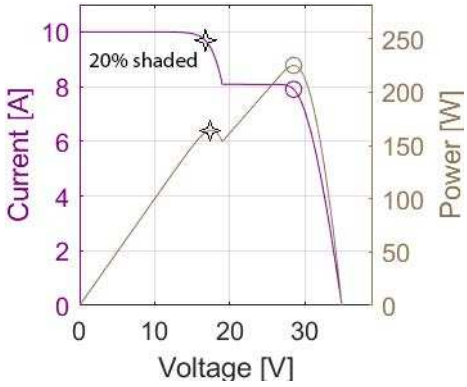

Figure 2: IV- and voltage-power-curve of a 250 Watt PV-module with three bypass-diodes with 20% cell shading in a single cell string. Additionally, the global I_{MPP} and P_{MPP} are visualised with circles and string inverter system tracked MPP with stars.

With the centralised MPPT of a conventional system with PV modules connected in series and the lack of control capabilities of voltage and current at the module-level, the string voltage is decreased, as the by-pass diodes of the shaded modules turn on. In certain cases, the shaded modules will then be operated in the lower power maximum. In the case of a system with power optimizers, the current and voltage of the shaded modules can be adjusted and set to the values of the global MPP of the module instead to a local one, while not influencing the values of the other modules. Consequently, the MLPE system will operate with a higher performance than the string inverter system, as long as the difference in performance is greater than the losses resulting from the additional conversion step (see Eq. 1).

$$(P_{MLPE,MPP} \cdot \eta_{DC/DC}) - P_{conv,MPP} > 0 \qquad (1)$$

It is important to identify the scenarios (i.e. share of shaded cell area) when the power optimizer operates at a higher performance. However, as soon as a shading of approximately $\geq 48\,\%$ of a cell string is reached, both systems will track the same MPP (as visualised in Figure 3 and Figure 4). Therefore, it can be identified as the maximum cell shade value for a possible increase in performance by the MLPE system [13].

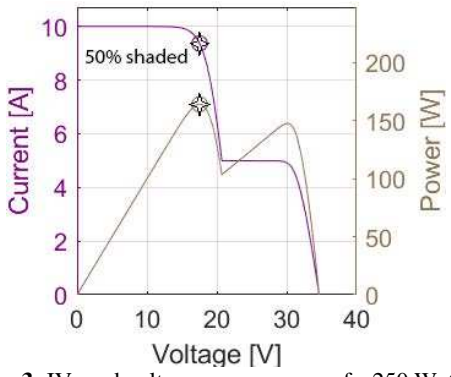

Figure 3: IV- and voltage-power-curve of a 250 Watt PV-module with three bypass-diodes with 50% cell shading in a single cell string. Additionally, the global I_{MPP} and P_{MPP} are visualised with circles and string-inverter system tracked MPP with stars.

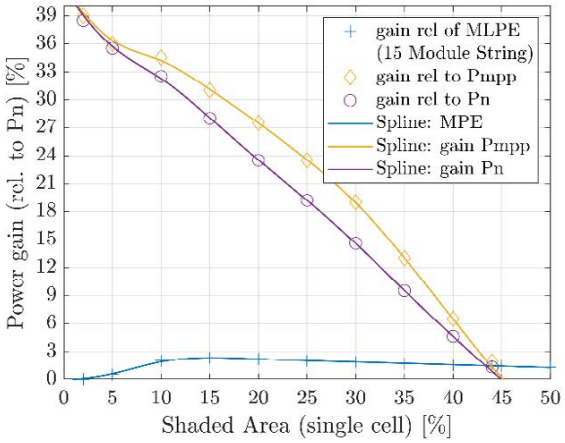

Figure 4: Plots and splines of the potential, relative MLPE system gains for shading of a single cell area in percent. Both, the module power gain relative to nominal module power (in violet) and the power gain relative to the power at the MPP (in yellow) are visualised. In blue, the relative total power gain of a MLPE system consisting of 15 modules in string.

Today, the CEC weighted efficiency is expected to be around 97 % for state-of-the-art string inverters [14]. Nowadays sophisticated switching devices (e.g. newly developed MOSFET and IGBT [15]) are used for power optimizer and therefore the efficiency can be very high with around 98.8% [16]. Furthermore, the mentioned efficiency depends on the voltage difference over the power optimizer. However, due to the adjustment of the DC-Voltage before the inverter, optimal values for the conversion can be set, resulting in an DC/AC conversion less dependent on the systems architecture and with efficiencies assumed to be closer to the peak efficiency given in the datasheet (e.g. 97.6 % [17]). Still, due to the additional conversion process, the system with power optimizers is more likely to have a lower total efficiency in unshaded operation (as shown in Eq. 2).

$$\begin{aligned} \Delta\eta_{str\text{-}MLPE} &= \eta_{conv,string} - \eta_{MLPE,tot} \\ &= \eta_{conv,string} - (\eta_{DC/AC} \cdot \eta_{DC/DC}) \\ &\approx 97\,\% - (97.6\,\% \cdot 98.8\,\%) \\ &= 97\,\% - 96.64\,\% \\ &= +\,0.36\,\% \end{aligned} \qquad (2)$$

3 LABORATORY SETUP

Table I: Measurement device 1-10 for MLPE

Name	N4L PPA1500 Precision Power Analyzer
Precision	Voltage measurement: 0.05 % Rdg + 0.1 % Rng + (0.005 % × kHz) +5 mV Current Measurement: 0.05 % Rdg + 0.1 % Rng + (0.005 % × kHz) +500 µA
Picture	

Table II: Measurement device 11 for Inverter

Name	N4L PPA5500 Precision Power Analyzer
Precision	Voltage measurement: 0.01 % Rdg + 0.038 % Rng + (0.004 % × kHz) + 1 mV Current Measurement: 0.01 % Rdg + 0.038 % Rng + (0.004 % × kHz) + 100 µA

Table III: Tested device 1-10 - Power Optimizer

Name	SE P405 Power Optimizer
Rated Input DC Power	405 W
Absolute Max. Input Voltage	125 Vdc
MPPT Operating Range	12.5V – 105V
Max. Short Circuit Current	10.1 Adc
Max. Efficiency	99.5 %
Weighted Efficiency	98.8 %
Max. Output Voltage	85 Vdc
Max. Output Current	15 Adc
Picture	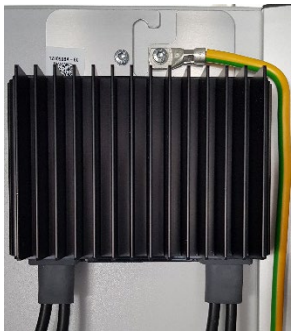

Table IV: Tested device 11 - PV-Inverter

Name	SE3500 Single Phase Inverter
Rated AC Output Power	3500 VA
Nominal AC Frequency	50 ± 5 Hz
AC Output Voltage	230 V
Max. Cont. Output Current	16 A
Max. DC Input Power	4700 W
Max. DC Input Voltage	500 Vdc
Nominal DC Input Voltage	350 Vdc
Max. Input Current	13.5 Adc
Maximum Inverter Efficiency	97.6 %
European weighted Efficiency	97.5 %
Picture	

Table V: Sources 1-10 - PV-Simulators

Name	Agilent E4362A Modular Solar Array Simulators
Rated Output DC Power	600 W
Max. DC Open-circuit Voltage	130V
Max. DC Output Voltage V_{MPP}	120 V
Max. short-circuit Current	5 A
Max. rated Current I_{MPP}	5 A
Picture	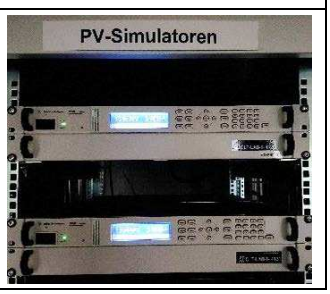

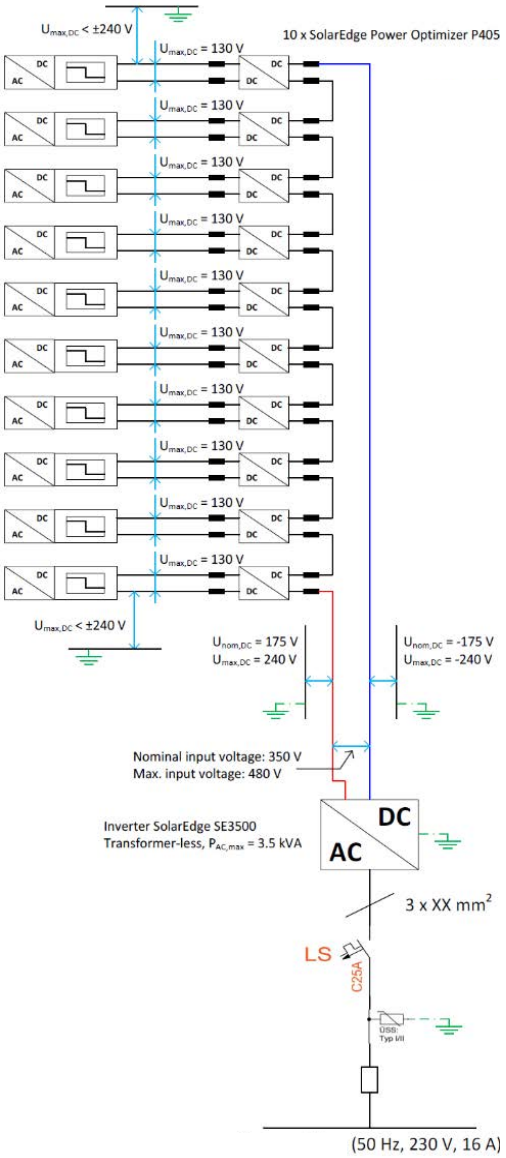

Figure 5: Electrical setup of the analysed MLPE system with 10 power optimizers.

4 ANALYSED CONDITIONS

4.1 Efficiency test

For the detailed analysis of the MLPE system efficiency, the fixed mode of the SAS was used to set static values in an interval of 5 seconds. In detail, a voltage range of 12 to 78 Volts with 2 V steps and a current range of 0.2 to 5 Ampère with 0.1 A steps was tested and evaluated. New SAS devices with a higher power rating will be installed and used in subsequent works to properly test and examine the efficiency.

4.2 Real-time irradiation test

To assess the performance of the power optimizer system over one day, the SAS devices received the values for I_{MPP}, I_{SC} and U_{MPP}, U_{OC} every 5 seconds, based on precalculated IV-curve values of a PV module. The testing was performed over 12.5 hours. The input IV curve data of the test are based on a clear-sky simulation of a PV system with 10 modules in heavy shaded conditions. An overview of the simulated system, the corresponding module placement and three shading conditions are visualised in Figure 6. Notably, the simulation used an inclination of 30 % with a module plane facing the south.

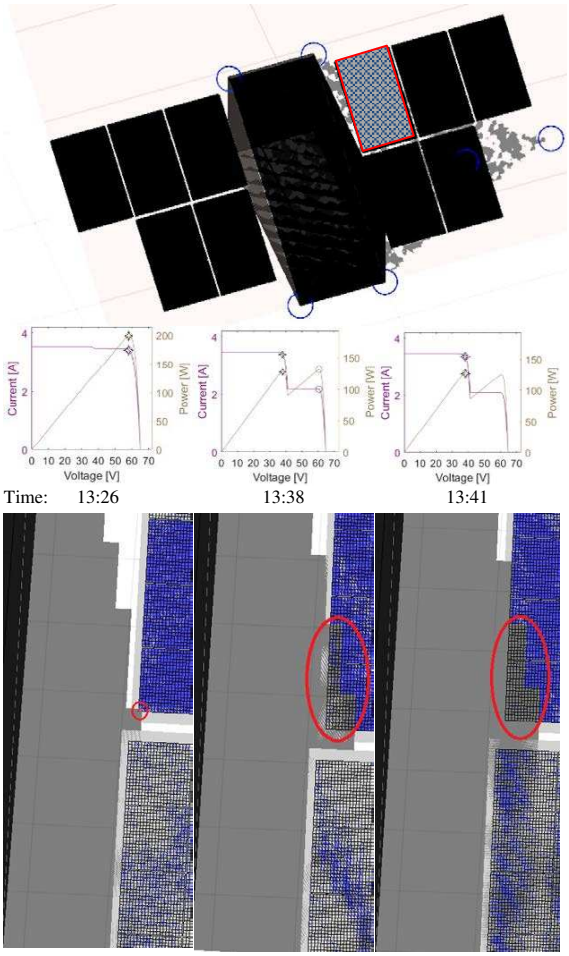

Figure 6: From top to bottom: The graphical representation of the simulated system of the real-time irradiation test. Additionally, the IV-curve of one module and graphical representation of three different shading situations (1%, 47% and 50% of one cell) of the simulated duration are visualised.

Furthermore, the sun path for the 20th March for Winterthur, Switzerland was used as input values. In accordance with the laboratory equipment used for the testing, modules with a maximum I_{MPP} of 5A were assumed for the simulation. Moreover, conditions with no shading only exist for a short duration, in this case 30 minutes, at solar noon for the simulated system.

5 MEASUREMENT RESULTS

For the evaluation of the total performance of the analysed MLPE system, the transformer-less PV inverter efficiency needed to be measured. As visualised in Figure 7, the inverter measurements were performed only under partial load conditions due to the limited power of the SAS in the lab. Nonetheless, a first approximation of the DC/AC conversion efficiency was reached, which shows the highest value of 97.4 % at 1336.2 W. Consequently, the difference to the datasheet value of 0.2 % [17] is below the measurement uncertainty.

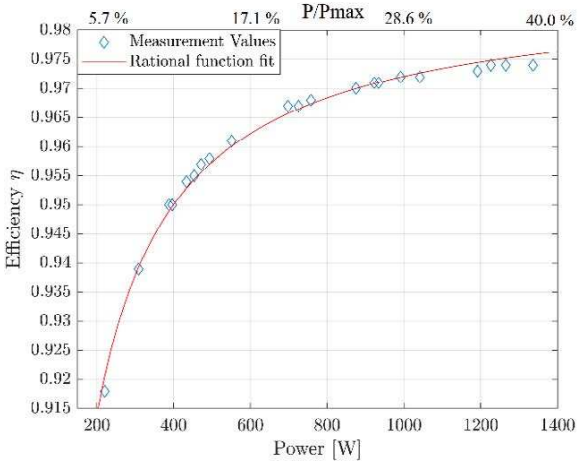

Figure 7: Measured efficiency values for the DC/AC conversion of the inverter of the MLPE-system in function of the power. Additionally, the rational function fit of the efficiencies is visualised as a curve.

As previously mentioned in Section 2, the efficiency of the DC/DC conversion of the power optimizer is important to determine when each PV system topology generates more power. In other words, it defines the power difference, which must be overcome by the additional yield gained from the operation of the power optimizers during shaded conditions. In Figure 8, the efficiency of the power optimizers is plotted as a function of module voltage and current to provide an overview of the electrical behaviour of the power optimizer. The grey points show the measurement values and the coloured surface represent the piecewise linear interpolation of the measured values, which improves the visibility of the voltage dependency of the efficiency, especially below 40 Volts. Similarly, the current shows an efficiency drop which is most evident at low voltage values.

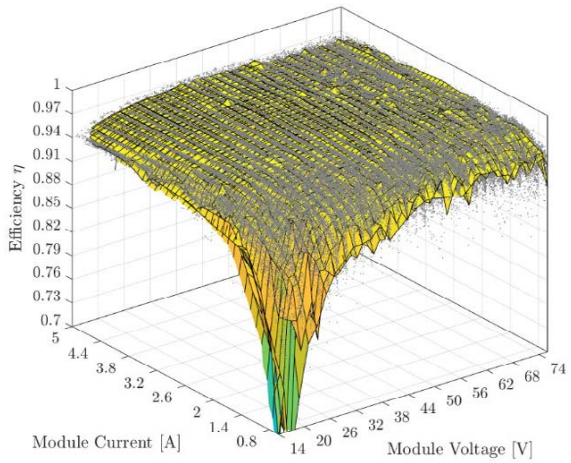

Figure 8: 3-D plot of the efficiency of the DC/DC conversion as a function of current and voltage values and interpolation of the values as visual aid.

The average efficiency value for each 1-Watt bin is visualised in Figure 9 and the maximum efficiency is found at 171 W with a value of 97.21%. The difference to the datasheet value of 2.29% is significant. However, due to the strong dependency of the efficiency of the DC/DC conversion on the input to output voltage ratio, the average values are not a general reference for every operating condition.

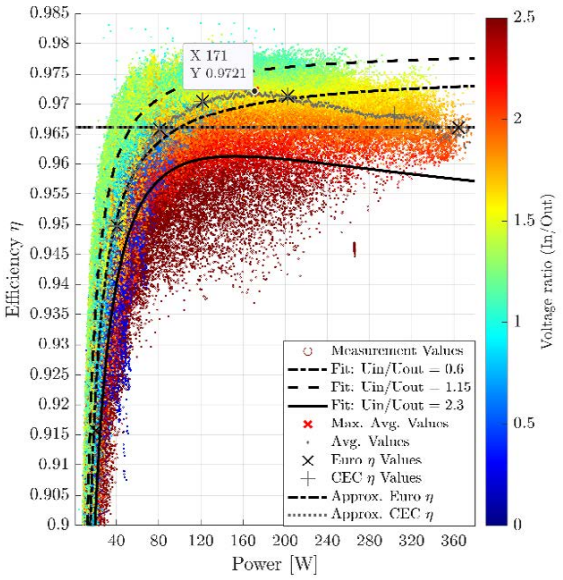

Figure 9: Efficiency values of the DC/DC conversion of the power optimizers as a function of the input power and voltage ratio (in/out) based colouring with colour bar.

Therefore, curve fitting for the measurement values for three different voltage ratios, namely, 0.6, 1.15 and 2.3, ± 0.1, were determined. As expected, the average efficiency values for a power of more than 180 W are influenced by the suboptimal voltage ratios of > 1.75. In addition, an approximated European and CEC efficiency was calculated, which uses the values at 90% of nominal power instead of at 100%, due to the limited power range of the SAS devices. Both values resulted in 96.61%, which is visualised in Figure 9 and indicated by the horizontal lines. Finally, highest efficiency values of 98% was measured in a narrow field at voltage ratios of 0.99 to 1.1.

In Figure 10, the power before and after the DC/DC conversion of the real-time irradiation test for four power optimizer is visualised, due to limited power range of the SAS devices, the curve was flattened between hour 10 and 14. Still, the effects of shading are most prominent between hour 7 and 10. Additionally, the resulting efficiency of the power optimizer is shown, whereby a plunge in efficiency in shaded conditions of approximately 5% to a value of 90 % in average can be discerned.

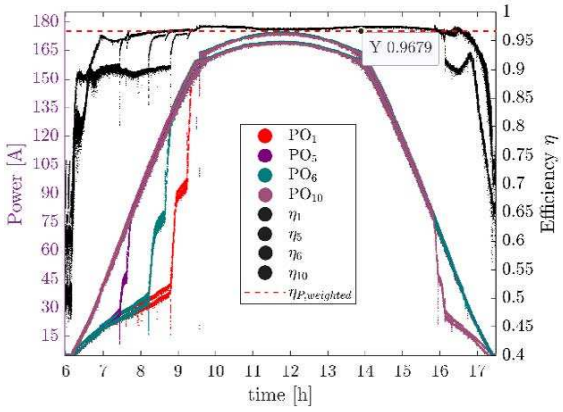

Figure 10: Plot of the real-time irradiance testing with input and output power of four power optimizers and respective efficiency values in function of time.

Additionally, to properly demonstrate the transients of the testing, the plot of the power values and according efficiencies from Figure 10 are visualised in Figure 11.

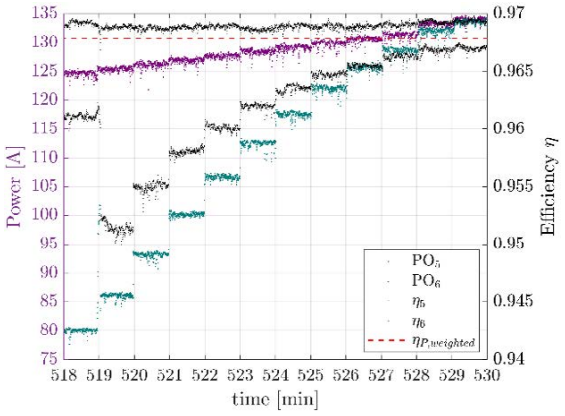

Figure 11: Detailed plot of the real-time irradiance testing transients of the input power of power optimizers 5 and 6, as well as their respective efficiency values over time.

In order to determine a performance rating of the system during realistic operating conditions, a weighted efficiency value was calculated at each timestep during the real-time test according to Formula 3.

$$\eta_{avg,wgt} = \frac{1}{N}\sum_{Opt=1}^{N}\frac{P_{out,N}(t)}{P_{out,mean,N}} * \eta_N(t) \qquad (3)$$

The resulting efficiency value is 96.79% as visualised by the dashed red line in Figure 10 and Figure 11. The efficiency can be expected to be slightly higher in the case with modules with a lower U_{MPP} (i.e. lower voltage ratio).

Due to the reason that the efficiency of the power optimizer varies greatly with the ratio of voltages, they were determined to and visualised in the Figure 12. Furthermore, the average voltage ratio is visualised with a value of 2.054 and the power weighted voltage ratio with a value of 1.586.

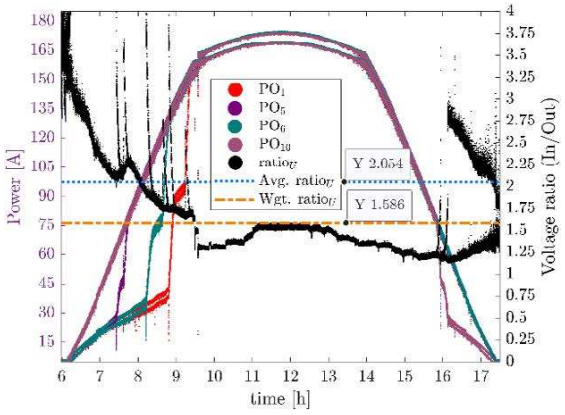

Figure 12: Plot of the real-time irradiance test with input and output power of four power optimizers and respective voltage ratio values in function of time.

6 DISCUSSION

The resulting efficiencies are only representative for a lower range of irradiance conditions. Nonetheless, a first approximation of performance of the devices were achieved and are presented in Table VI.

Table VI: Resulting efficiency values of the devices

Name	Device	Measured	Difference to datasheet	Unit
DC/AC η	SE3500	97.4	0.20	%
DC/DC Max Avg η	P405	97.21	2.29	%
DC/DC Pow. wgt. η	P405	96.79	2.71	%
DC/DC Euro & CEC η	P405	96.61	2.89	%

Finally, the resulting efficiencies of the power optimizer and the PV-inverter were multiplied, and therefore, the total system performance estimated, which are stated in Table VII.

Table VII: Total performance of the MLPE system

Name	Resulting total system η	Unit
Total Max Avg η	94.78	%
Total Power weighted η	94.37	%
Total European & CEC η	94.19	%

Due to the limited power range of the SAS devices, an increased voltage and lower current was used during the testing. This has the potential to reduce the efficiency values of the power optimizers. Still, the total system performance value (e.g. the total power weighted efficiency) shows a significant deviation of approximately -2.27 % from the potential efficiency, estimated by the combined MLPE system datasheet values.

If there is a specific shading situation, the benefit of MLPE, must be determined on a case-by-case basis. There is not a general statement available for all cases. As for the simulated PV system, an additional daily yield of approximately 3.5 % was calculated for the use of MLPE. The results of the simulation are stated in Table VIII.

Table VIII: Simulation result of a clear-sky day with the sun path of the 20th March at Winterthur, Switzerland, and updated efficiency values for the system with MLPE

System type	Weighted system η	Simulated Daily yield	Unit
MLPE	94.37	103.5	%
String inverter	97.00	100.0	%

In scenarios with extreme shading a MLPE system provides a significant advantage. Whereas for low shading situations, such systems are generally expected to yield less energy than conventional systems. On the other hand, the placement of the shade on the module is of key importance. As for example, a shade, which is orthogonal to the cell strings (as in the simulation), will lead to significant losses in a conventional system. Accordingly, various shading situations must be examined with the indoor test facility presented in this paper. Consequently, environmental impacts are reduced, and exact performance results determined, which would not be possible by using outdoor testing facilities.

ACKNOWLEDGEMENT

This paper is part of the ongoing research by IEA Smart Grid International Research Facility Network (SIRFN) [18]. Notably, it is part of IEA Task 13 [19] and funded by the Swiss Federal Institute of Energy in projects BFE Nr. SI501524-01 and BFE SFOE8100073.

REFERENCES

[1] H. Kolm, "Photovoltaic alternating current generator has solar modules, each electrically connected to individual D.C. voltage converter that transforms to intermediate D.C. voltage and decouples module," German Patent DE10136147A1, Jul. 25, 2001.

[2] W. F. Capp and W. J. Driscoll, "Power converter for a solarpanel," U.S. Patent US20070103108A1, May 27, 2004.

[3] P. Wolfs, "Device for distributed maximum power tracking for solar arrays," U.S. Patent US7839022B2, Jul. 12, 2005.

[4] SolarEdge Technologies Ltd. "SolarEdge Introduces First PV Power Harvesting System to Maximize Power Generation of Each Module Throughout the Solar Lifecycle." solaredge.com. https://www.solaredge.com/us/content/solaredge-scores-over-15mw-pv-power-optimizer-system-orders-german-market-during-intersolar (accessed Jul. 22, 2020).

[5] A. Gupta and A. S. Bais, "Power Optimizer Market Market Share & Forecast, 2019 – 2025," GMI Inc., Selbyville, DE, USA, Rep. GMI3075, Jan. 2019. Accessed: Aug. 3, 2020. [Online]. Available: https://www.gminsights.com/industry-analysis/power-optimizer-market

[6] M. De Jesus. "Record shipments push global solar PV inverter market past $9 billion in 2019." pv-magazine.com. https://www.pv-magazine.com/2020/06/25/record-shipments-push-global-solar-pv-inverter-market-past-9-billion-in-2019/ (accessed Aug. 3, 2020).

[7] SolarEdge Technologies Inc. "Solaredge Fact Sheet." solaredge.com. https://www.solaredge.com/sites/default/files/se-fact-sheet-na.pdf (accessed Jul. 27, 2020).

[8] M. Osborne. "SolarEdge sales reach US$271.9 million in Q1 on strong demand from Europe." pvtech.com. https://www.pv-tech.org/news/solaredge-sales-reach-us271.9-million-in-q1-on-strong-demand-from-europe (accessed Jul. 28, 2020).

[9] G. R. Walker and P. C. Sernia, "Cascaded DC–DC Converter Connection of Photovoltaic Modules," *IEEE Trans. Power Electr.*, vol. 19, no. 4, pp. 1130-1139, Jul. 2004, doi: 10.1109/TPEL.2004.830090.

[10] R. Alonso et. al., "Analysis of performance of distributed architectures based on dc-dc converters," in *Proc. 25th EU PVSEC / 5th WCPEC*, Valencia, Spain, Sep. 6-10, 2010, pp. 4454-4458.

[11] C. Deline et. al., "Photovoltaic Shading Testbed for Module-Level Power Electronics: 2016 Performance Data Update," National Renewable Energy Laboratory (NREL), Golden, Colorado, United States of America, Rep. TP-5J00-62471, Sep. 2016. Accessed: Jul. 12, 2020. [Online]. Available: https://www.nrel.gov/docs/fy16osti/62471.pdf

[12] M. Calais and V. G. Agelidis, "Multilevel converters for single-phase grid connected photovoltaic systems-an overview," in *Proc. IEEE Int. Symp. Indust. Electr. (ISIE'98)*, Jul. 7-10, 1998, pp. 224-229.

[13] F. Baumgartner et al., "Effizienzvergleich PV-String-Inverter versus dezentrale PV-Modulelektronik," in *18. National PV Conference Switzerland*, Lausanne, Mar. 13, 2020. [Online]. Available: home.zhaw.ch/~bauf/

[14] California Energy Commission (CEC), "Solar equipment list: Grid support inverter list – full data." Aug. 21, 2020. Distributed by the Solar Equipment Center of the California Energy Commission. [Online]. Available: https://www.energy.ca.gov/programs-and-topics/topics/renewable-energy/solar-equipment-lists

[15] S. Kouro, J. I. Leon, D. Vinnikov and L. G. Franquelo, "Grid-Connected Photovoltaic Systems: An Overview of Recent Research and Emerging PV Converter Technology," in *IEEE Industrial Electronics Magazine*, vol. 9, no. 1, pp. 47-61, March 2015, doi: 10.1109/MIE.2014.2376976.

[16] SolarEdge Technologies, Ltd., "Power Optimizer: P300 / P370 / P404 / P405 / P500 / P505," Aug. 2019. [Online]. Available: https://www.solaredge.com/sites/default/files/se-p-series-add-on-power-optimizer-datasheet.pdf

[17] SolarEdge Technologies, Ltd., "SolarEdge Single Phase Inverters-16A: SE3000(*)(**) / SE3500(*)(**) / SE4000-16A," Nov. 2016. [Online]. Available: https://www.solaredge.com/sites/default/files/se-single-phase-16a-inverter-datasheet.pdf

[18] IEA Smart Grid International Research Facility Network (SIRFN), "Participants". [Online]. Available: http://www.sirfn.net/participants/

[19] International Energy Agency (IEA), "Task13". [Online]. Available: http://www.iea-pvps.org/index.php?id=57#c90